Cited2 is required both for heart morphogenesis and establishment of the left-right axis in mouse development

Wolfgang J. Weninger[1,*,†], Kylie Lopes Floro[2,*], Michael B. Bennett[3], Sarah L. Withington[2], Jost I. Preis[2], Juan Pedro Martinez Barbera[4], Timothy J. Mohun[3] and Sally L. Dunwoodie[2,5,†]

[1]Integrative Morphology Group, Department of Anatomy, University of Vienna, Waehringerstrasse 13, A-1090 Vienna, Austria
[2]Developmental Biology Program, The Victor Chang Cardiac Research Institute, 384 Victoria Street, Darlinghurst, NSW 2010, Australia
[3]Developmental Biology Division, National Institute for Medical Research, The Ridgeway, Mill Hill, London NW7 1AA, UK
[4]The Neural Development Unit, The Institute of Child Health, 30 Guilford Street, London WC1N 1EH, UK
[5]St Vincent's Clinical School, and School of Biotechnology and Biomolecular Sciences University of New South Wales, Kensington, NSW, Australia
*These authors contributed equally to this work
†Authors for correspondence (e-mail: wolfgang.weninger@meduniwien.ac.at; s.dunwoodie@victorchang.unsw.edu.au)

Accepted 4 January 2005

Development 132, 1337-1348
Published by The Company of Biologists 2005
doi:10.1242/dev.01696

Summary

Establishment of the left-right axis is a fundamental process of vertebrate embryogenesis. Failure to develop left-right asymmetry leads to incorrect positioning and morphogenesis of numerous internal organs, and is proposed to underlie the etiology of several common cardiac malformations. The transcriptional modulator Cited2 is essential for embryonic development: *Cited2*-null embryos die during gestation with profound developmental abnormalities, including cardiac malformations, exencephaly and adrenal agenesis. *Cited2* is also required for normal establishment of the left-right axis; we demonstrate that abnormal heart looping and right atrial and pulmonary isomerism are consistent features of the left-right-patterning defect. We show by gene expression analysis that *Cited2* acts upstream of *Nodal*, *Lefty2* and *Pitx2* in the lateral mesoderm, and of *Lefty1* in the presumptive floor plate.

Although abnormal left-right patterning has a major impact on the cardiac phenotype in *Cited2*-null embryos, laterality defects are only observed in a proportion of these embryos. We have therefore used a combination of high-resolution imaging and three-dimensional (3D) modeling to systematically document the full spectrum of *Cited2*-associated cardiac defects. Previous studies have focused on the role of *Cited2* in cardiac neural crest cell development, as Cited2 can bind the transcription factor Tfap2, and thus affect the expression of Erbb3 in neural crest cells. However, we have identified *Cited2*-associated cardiac defects that cannot be explained by laterality or neural crest abnormalities. In particular, muscular ventricular septal defects and reduced cell density in the atrioventricular (AV) endocardial cushions are evident in *Cited2*-null embryos. As we found that *Cited2* expression tightly correlated with these sites, we believe that *Cited2* plays a direct role in development of the AV canal and cardiac septa. We therefore propose that, in addition to the previously described reduction of cardiac neural crest cells, two other distinct mechanisms contribute to the spectrum of complex cardiac defects in *Cited2*-null mice; disruption of normal left-right patterning and direct loss of *Cited2* expression in cardiac tissues.

Key words: Cited2, Left-right axis, Heart development, Mouse

Introduction

Cardiac morphogenesis understandably relies on genes that function within the heart, but many genes extrinsic to the heart also affect its development. Genes required to establish the left-right axis of the embryo indirectly affect heart morphogenesis. They do this by ultimately affecting the expression of the *Pitx2* gene (Burdine and Schier, 2000; Franco and Campione, 2003; Hamada et al., 2002). It is the *Pitx2c* isoform that is central to the establishment of laterality; it is expressed in left lateral plate mesoderm (LPM), and later expression in the left side of the heart is considered to extend from this (Campione et al., 2001). *Pitx2c* is a Nodal-responsive gene and thus its expression in the left LPM occurs as a direct consequence of Nodal signaling in the tissue. *Nodal* expression in the left LPM, establishes the left side of the embryo, and so genes required to initiate, maintain and restrict the expression of *Nodal* are all required for correct *Pitx2c* expression.

The *Cited2* gene affects cardiac morphogenesis and was identified from studies of differential gene expression in the early embryo (Dunwoodie et al., 1998), cytokine function (Sun et al., 1998) and transcriptional regulation during hypoxia (Bhattacharya et al., 1999). *Cited2* expression is widespread during early mouse and chicken development (Dunwoodie et al., 1998; Schlange et al., 2000). Furthermore, expression of *Cited2* can be activated by factors, including low oxygen tension, cytokines, lipopolysacharide and shear stress (Bhattacharya et al., 1999; Sun et al., 1998; Yokota et al.,

2003). This may account for the complexity of expression in developing embryos.

Cited2 interacts with CBP and p300 – homologous proteins with intrinsic acetyltransferase and E4 ubiquitin ligase activities (Chan and La Thangue, 2001; Grossman et al., 2003). It inhibits the transcriptional activity of Hif1α, through competition for overlapping binding sites on CBP/p300 (De Guzman et al., 2004; Freedman et al., 2003). This may represent a paradigm for Cited2 function, as it also appears to displace Ets1 from CBP/p300 (Yokota et al., 2003). In addition, Cited2 interacts directly with the transcription factors Lhx2 and Tfap2 (Bamforth et al., 2001; Glenn and Maurer, 1999).

Cited2-null embryos display numerous developmental defects (Bamforth et al., 2001; Martinez Barbera et al., 2002; Yin et al., 2002). Cardiac defects previously reported in *Cited2*-null embryos include: double outlet right ventricle (DORV); atrial septal defect (ASD); ventricular septal defect (VSD); overriding aorta; persistent truncus arteriosus (PTA); and pulmonary artery stenosis. Previously, these defects had only been considered in light of Tfap2 and Hif1α, and were only described at late stages of gestation (13.5 dpc onwards) when the heart has essentially reached its final morphology (Bamforth et al., 2001; Martinez Barbera et al., 2002; Yin et al., 2002). We determined the developmental origins of the cardiac defects by examining cardiac morphogenesis in detail at a number of embryonic stages, and determined the expression pattern of *Cited2* in relation to heart development.

We observed that the heart loops abnormally in a proportion of *Cited2*-null embryos, and that these embryos have right atrial isomerism (RAI). In these embryos, *Nodal*, *Lefty2* and *Pitx2c* are not expressed in lateral mesoderm, and *Lefty1* expression in the prospective floor plate (PFP) is abnormal. This shows that abnormal left-right patterning has a major impact on the cardiac phenotype in *Cited2*-null embryos. In addition, we performed a detailed analysis of the endpoint cardiac phenotypes using episcopic fluorescence image capturing (EFIC) and three-dimensional (3D) modeling. A number of abnormalities were identified in *Cited2*-null embryos that lacked a laterality defect, and some of these were consistent with a reduction in cardiac neural crest (CNC) cells. There were, however, two defects that did not seem to relate to abnormalities in laterality or CNC cells: reduced cell density in the AV endocardial cushions and muscular ventricular septal defects (VSD). These defects did, however, directly correlate with *Cited2* expression and this suggests that *Cited2* also plays a direct role in cardiac tissue.

In summary, we demonstrate that *Cited2*-null embryos display a spectrum of cardiovascular defects: some consistent with a laterality defect, others with a reduction in neural crest cells and yet others concordant with *Cited2* acting directly within cardiac tissue to affect morphogenesis.

Materials and methods

Mouse lines and genotyping

The *Cited2-lacZ* mouse line (Barbera et al., 2002) is maintained on a C57BL/6;129 hybrid genetic background following three backcrosses onto C57BL/6. Mice heterozygous for this *Cited2* targeted allele (*Cited2*$^{+/-}$) were intercrossed to produce *Cited2* wild-type (*Cited2*$^{+/+}$), heterozygous (*Cited2*$^{+/-}$) and homozygous null (*Cited2*$^{-/-}$) embryos for analysis. *Cited2* heterozygous mice were also crossed with mice homozygous for the *MLC3F-nlacZ-2E* transgene, which is maintained on a SJL;C57BL/6 hybrid genetic background (Kelly et al., 1995).

Morphology, histology, RNA in situ hybridization and X-gal staining

EFIC was used for high resolution morphological studies (Weninger and Mohun, 2002). Histology, RNA in situ hybridization and X-gal staining were performed as described (Kaufman, 1992; Hogan et al., 1994; Harrison et al., 1995). cDNA probe details are as follows: *Cited2* (Dunwoodie et al., 1998); *Nodal*, *Lefty1/2* and *Pitx2c* probes were a gift from Christine Biben and Richard Harvey.

Determination of cell density in endocardial cushions

Cell density of the AV cushions was measured in three *Cited2* wild-type and three *Cited2*-null embryos at 10.5 dpc. Wax sections of each embryo were cut at a 45° angle (midway between frontal and transverse) and every section collected. The number of cells in the central section plus two before and two after the central section were counted. Cushion area was measured using Image J software v1.24o (NIH), and the results expressed as density of cells per μm^2 cushion. Cell density was compared using analysis of variance.

Scanning electron microscopy (SEM)

Following incubation in Karnovsky's fixative (2% paraformaldehyde, 2.5% glutaraldehyde and 0.1 M sodium phosphate buffer at pH 7.2), SEM was performed (Webb et al., 1998).

Results

Cited2 is expressed in the heart and elsewhere in the embryo

The cardiovascular defects previously identified in *Cited2*-null embryos have been ascribed to a reduction in CNC cells or impaired Hif1α activity (Bamforth et al., 2001; Martinez Barbera et al., 2002; Yin et al., 2002). *Cited2* was expressed in a number of sites within the embryo that could impact on the development of the heart (Fig. 1). *Cited2* at 7.5 dpc was expressed in the ventral node, predominantly in the caudal lip but also in the depression of the node (Fig. 1A-C) (Dunwoodie et al., 1998). Expression was readily detected in 8 dpc embryos in the cardiac crescent, anterior lateral mesoderm and in trunk paraxial mesoderm (Fig. 1C-F). At 9.25 dpc, expression was elevated in dorsal neuroectoderm at the forebrain-midbrain boundary, and in the hindbrain (Fig. 1G,H). Expression was also readily detected in branchial arches 1 to 3, and in somites. At this stage, in the heart, *Cited2* expression was widespread: elevated levels of expression were identified in the aortic sac, in the myocardium adjacent to the endocardial cushions of the outflow tract and the AV canal, and in the presumptive atria and sinus venosus (Fig. 1G,I-K). At 10.5 dpc, elevated *Cited2* expression was detected in branchial arch 4, the outflow tract and the AV canal (Fig. 1L-N). At 13.5 dpc *Cited2* expression was largely restricted to the outflow and inflow regions of the heart, AV cushion, septum primum and the tip of the muscular ventricular septum (Fig. 1O-Q). With respect to expression in the heart, *Cited2* is found predominantly in the myocardium; however, some endocardial cells, and cells within the endocardial cushion, also express the gene.

Abnormal heart looping and atrial isomerism are features of the Cited2 null phenotype

Cited2-null embryos die from 14.5 dpc (Table 1). Examination of *Cited2*-null hearts between 9.5 and 12.5 dpc, revealed that

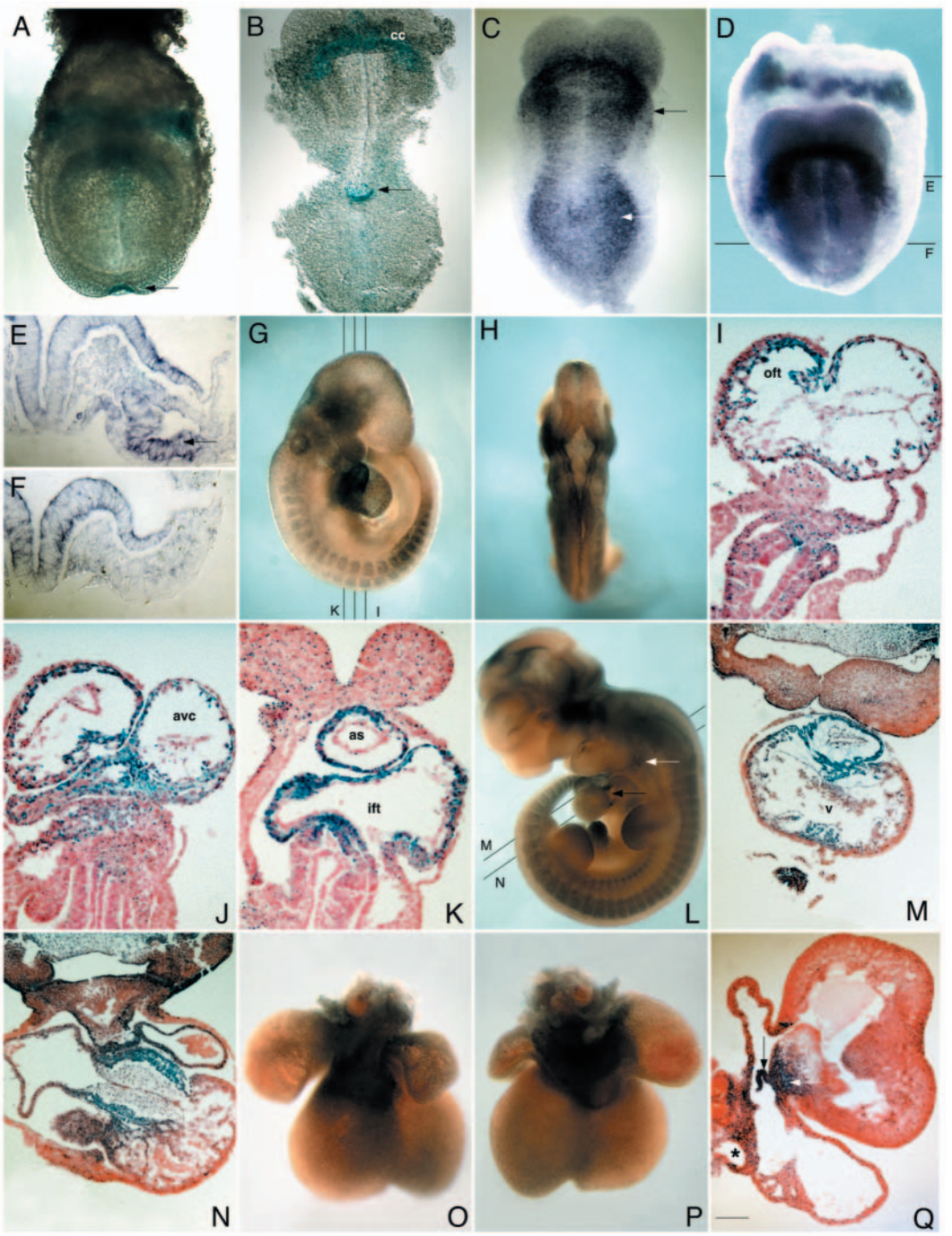

Fig. 1. *Cited2* is differentially expressed in the heart and elsewhere during development. (A) Anterior view of a late headfold stage embryo (7.5 dpc) showing expression in the ventral node (arrow), cardiac crescent and blood islands. (B) Ventral view of a flatmounted four-somite stage embryo (8 dpc) showing expression in the cardiac crescent and in the caudal lip and pit of the node (arrow). (C) Ventral view of a flatmounted six-somite stage embryo (8 dpc) showing expression in the cardiac crescent, anterior lateral mesoderm (black arrow), paraxial mesoderm (white arrow) and node. (D) Anterior view of a six-somite stage embryo showing elevated expression in the cardiac crescent, anterior lateral mesoderm and trunk paraxial mesoderm. (E,F) Transverse sections through D at the levels indicated showing elevated expression in the cardiac mesoderm (arrow) and low-level expression throughout. (G) Lateral and dorsal view of 21-somite stage embryo (9.5 dpc) showing elevated expression in the forebrain-midbrain boundary, branchial arches 1 and 2, heart, and somites. (H) Dorsal view of the embryo in G showing expression in the hindbrain (rhombomeres 3, 5, 6, 7) and adjacent paraxial mesoderm. (I-K) Frontal sections through a 21-somite stage embryo at the levels indicated in G. (I) Expression is elevated in the ventricular myocardium and trabeculae of the outflow tract and presumptive right ventricle; (J) in the myocardium and, to a lesser extent, the endocardium and endocardial cushion cells in the outflow tract and atrioventricular canal; and (K) in the aortic sac, presumptive atria and sinus venosus (inflow tract). (L) Lateral view of 40-somite stage embryo (10.5 dpc) showing expression in the outflow tract, atrioventricular canal (black arrow), branchial arch 4 (white arrow), central nervous system, somites and limbs. (M,N) Sections through a 40-somite stage embryo at the levels indicated in L, showing: expression in the (M) outflow tract and, to a lesser extent, in the compact myocardium and trabeculae of the ventricles; and expression in the (N) myocardium adjacent to the endocardial cushion of the atrioventricular canal. (O) Ventral and (P) dorsal views of a heart dissected from an embryo at 13.5 dpc showing expression predominantly in the outflow tract (O) and inflow region (P). (Q) Frontal section through a dissected heart at the same stage as shown in O,P showing expression in the septum primum (black arrow), around the vena cava (asterisk) and in the endocardial cushions of the atrioventricular canal (white arrow). *Cited2* expression was assayed by detecting β-galactosidase activity from the *Cited2-lacZ* allele in embryos heterozygous (A,B,G,H,L,O,P) or homozygous (I,J,K,M,N,Q) for the allele, or via *Cited2* RNA hybridization (C-F). The colorimetric reaction used to identify *Cited2* transcripts was extended for the embryo in D, in order to reveal low levels of *Cited2* expression. cc, cardiac crescent; oft, outflow tract; ift, inflow tract; v, ventricle; avc, atrioventricular canal; as, aortic sac. Scale bar: 135 μm in A,B; 260 μm in C,D,H; 35 μm in E,F; 280 μm in G; 50 μm in I-K; 550 μm L; 94 μm in M,N; 390 μm O,P; 310 μm Q.

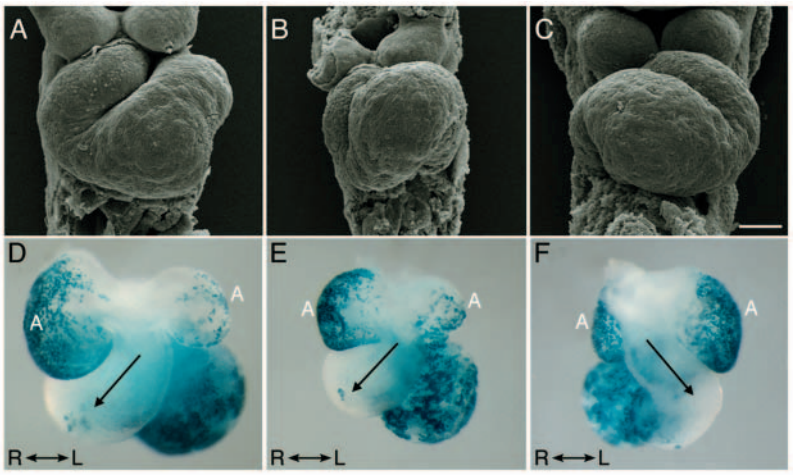

Fig. 2. *Cited2*-null hearts display cardiac looping defects and atrial isomerism. (A-C) Scanning electron micrographs showing ventral views of hearts at 9.5 dpc (23 somites). The head, tail and the pericardium were removed. (A) *Cited2* wild-type heart showing a normal D (rightward) loop. (B) *Cited2*-null heart showing an abnormal D loop. The left ventricle is ventrally displaced and occupies a more central position than normal. (C) *Cited2*-null heart showing an abnormal L (leftward) loop. (D-F) Right atrial isomerism is observed in *Cited2*-null embryos with abnormal heart loops. Ventral views of hearts from 10.5 dpc show expression of the *MLC3F-nlacZ-2E* transgene. (D) A *Cited2* wild-type heart shows a normal D (rightward) loop and asymmetric *MLC3F-nlacZ-2E* transgene. (E) A *Cited2*-null heart shows a normal D loop and asymmetric *MLC3F-nlacZ-2E* transgene. (F) A *Cited2*-null heart shows an L (leftward) loop and strong bilateral expression of the *MLC3F-nlacZ-2E* transgene, indicating right atrial isomerism. Arrows indicate orientation of the outflow tract. A, atrium; R L, right-left axis. Scale bar: 100 μm.

looping was abnormal (Fig. 2). All *Cited2* wild-type (*n*=167) and heterozygous (*n*=203) embryos had normal rightward (D) looping hearts (Fig. 2A). By contrast, almost half (52/115) of all *Cited2*-null embryos showed abnormalities in heart looping (Fig. 2B,C): 12 had abnormal D-looped hearts, while 40 had leftward (L) looped hearts. In most L-looped hearts, the ventricles were positioned on the left side of the midline of the embryo, while in abnormal D-looped hearts, both ventricles were on the right side of the midline. These looping defects indicated that specification of the left-right axis might not have occurred correctly in the *Cited2*-null embryos. To address this, we used the *MLC3F*-enhancer transgene that marks the right atrium (Franco et al., 2001; Kelly et al., 1998). At 10.5 dpc, all *Cited2* wild-type (*n*=69; Fig. 2D) and heterozygous embryos (*n*=61; data not shown) showed characteristic transgene expression in the right atrium, as did *Cited2*-null embryos with correctly looped hearts (*n*=13; Fig. 2E). By contrast, RAI, detected by bilateral expression of the *MLC3F*-enhancer transgene, was apparent in all *Cited2*-null embryos with an abnormally looped heart (*n*=15 for abnormal L-loops and *n*=6 for abnormal D-loops; Fig. 2F). These results demonstrate that the cardiac looping defects prevalent in *Cited2*-null embryos are concordant with RAI. In all *Cited2* null-embryos with RAI (*n*=14), we found right pulmonary isomerism (RPI): four lung lobes on both sides, as apposed to the normal arrangement with one lung lobe on the left and four on the right. In contrast to the thoracic isomerism, there was incomplete penetrance of abdominal isomerism: the stomach instead of lying normally on the left, was in the midline or on the right hand side (*n*=8/14).

Table 1. Genotype of mice resulting from *Cited2* heterozygous intercross on a mixed C57BL6:129 genetic background

	Genotype			
Stage	*Cited2*$^{+/+}$	*Cited2*$^{+/-}$	*Cited2*$^{-/-}$	*P*
8.5 dpc	68	184	100	0.0379
9.5 dpc	36	80	29	0.3283
10.5 dpc	36	84	31	0.3255
11.5 dpc	30	76	28	0.2897
12.5 dpc	14	23	10	0.7039
13.5 dpc	13	22	10	0.8097
14.5 dpc	106	159	85 (+6 dead)	0.0657
15.5 dpc	14	19	8 (+5 dead)	0.3724
16.5 dpc	5	12	8 (+1 dead)	0.6839
17.5 dpc	3	4	1	0.6065
PD21	402	615	0	<0.0001

Ratios of genotypes were tested for goodness of fit to expected Mendelian segregation (1:2:1) by χ^2 analysis, calculated with two degrees of freedom. *P* value calculated at 14.5, 15.5 and 16.5 dpc for living embryos only.
dpc, days post coitum; PD, postnatal day.

Determinants of laterality are abnormally expressed in a proportion of *Cited2*-null embryos

In order to examine the relationship of *Cited2* with other genes involved in specifying left-right identity, we examined *Nodal* expression. *Nodal* was asymmetrically expressed in the left LPM in *Cited2* wild-type (*n*=6) and heterozygous (*n*=12) embryos, and bilaterally expressed within the node (Fig. 3A,B). By contrast, two out of six *Cited2*-null embryos lacked *Nodal* expression in the left LPM (Fig. 3C). However, *Nodal* expression within the node was comparable with that in the controls. This suggests that *Cited2* is required for initiation or maintenance of *Nodal* expression in the LPM, but not within the node.

Lefty1 and *Lefty2* interact with Nodal and its co-receptors (cripto and cryptic) to block Nodal signaling (Chen and Shen, 2004; Cheng et al., 2004; Hamada et al., 2002). *Lefty2* is expressed in the left LPM and is a direct target of *Nodal* (Meno et al., 1997; Meno et al., 1996; Saijoh et al., 1999; Saijoh et al., 2000). *Lefty1* is expressed in the left side of the PFP but, unlike *Nodal*, *Lefty2* and *Pitx2c*, its expression is independent of Foxh1. Despite this, the reliance of *Lefty1* expression on Cryptic suggests that Nodal and/or Gdf1 are important for *Lefty1* expression (Hamada et al., 2002; Yan et al., 1999). As loss of *Nodal* expression in the LPM is a feature of the *Cited2*-null phenotype, we would expect a proportion of *Cited2*-null embryos to lack *Lefty1* and *Lefty2* expression. *Lefty1* and *Lefty2* were expressed normally in *Cited2* wild-type (*n*=13), heterozygous (*n*=17) and some *Cited2*-null (*n*=5) embryos (Fig. 3D,E,G,H). However, a proportion of *Cited2*-null embryos (*n*=4) lacked *Lefty2,* and expression of *Lefty1* was limited to and maintained in the posterior PFP (Fig. 3F,I). Expression of *Shh* is normal in the midline of all *Cited2*-null embryos, precluding the possibility that the embryonic midline is compromised (data not shown). Persistent posterior

expression of *Lefty1* in the PFP has not been previously reported in laterality mutants; this demonstrates that *Cited2* affects the establishment of laterality differently to any known gene.

Pitx2c is initially expressed in the left LPM, and then at later stages expression persists on the left side of various LPM-derived tissues such as the sinus venosus, common atrial chamber, cardinal vein, vitelline vein, septum transversum and foregut (Yoshioka et al., 1998). In all *Cited2* wild-type (n=6) and heterozygous (n=37) embryos examined, the normal pattern of *Pitx2c* expression was observed in the left LPM and later the left horn of the sinus venosus (Fig. 3J,K). However, in four out of 12 *Cited2*-null embryos, *Pitx2c* expression was entirely absent from this left lateral mesoderm (Fig. 3L). This indicates that *Cited2* acts upstream of *Pitx2c* expression in lateral mesoderm and is consistent with the fact that *Pitx2c* is not expressed because of an absence of *Nodal* expression in the lateral mesoderm.

In summary, one-third of *Cited2*-null embryos showed loss of *Nodal*, *Lefty2* and *Pitx2c* expression in left LPM, and loss of *Lefty1* expression in the anterior PFP; this is consistent with the proportions of null embryos, which had RAI (Table 2).

Pitx2c expression is Nodal responsive, its expression relies on Foxh1-binding sites in the left side-specific enhancer (ASE), and expression in the heart requires its earlier expression in the lateral mesoderm (Shiratori et al., 2001). Despite the fact that *Pitx2c* expression in the heart has never been shown to be uncoupled from its expression in the lateral mesoderm, we examined *Pitx2c* expression in *Cited2*-null hearts at 13.5 and 14.5 dpc to explore this possibility. *Pitx2c* expression was readily detected in hearts dissected from *Cited2* wild-type (n=4), heterozygous (n=6) and

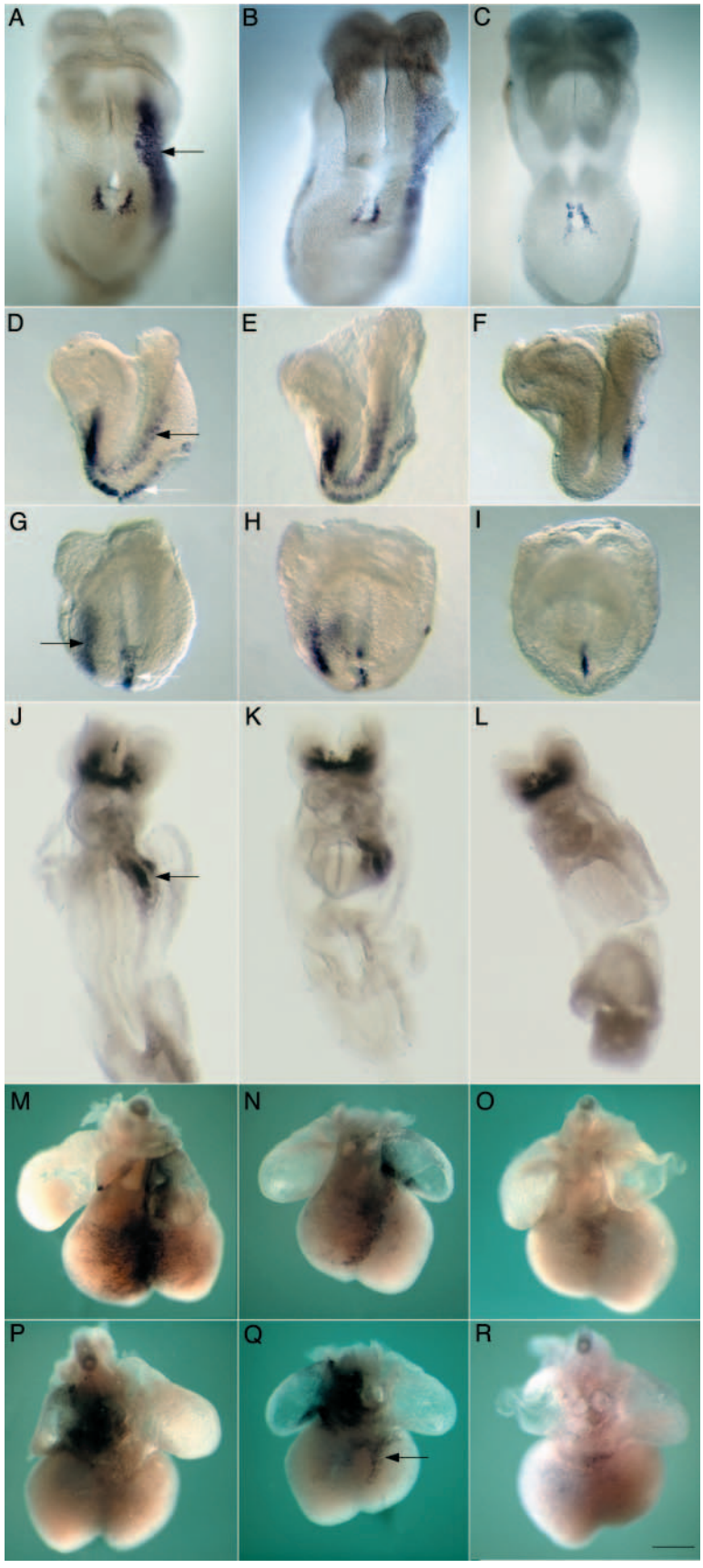

Fig. 3. *Cited2*-null embryos have abnormal expression of left sided determinants. RNA in situ hybridization of embryos and hearts hybridized with probes that recognize *Nodal* (A-C), both *Lefty1* and *Lefty2* (D-I), and *Pitx2* (J-R) transcripts. *Nodal* is expressed in the left lateral mesoderm (arrow) and node of six- to seven-somite stage *Cited2* wild-type (A) and heterozygous (B), but not in LPM of *Cited2*-null (C) embryos. (D-I) A combined *Lefty1/2* probe shows that *Lefty1* and *Lefty2* are expressed in the left prospective floor plate of the neural tube (white arrow), and left LPM (black arrow) respectively, in seven- to nine-somite stage *Cited2*-wild-type (D,G) and heterozygous (E,H) embryos. In *Cited2*-null embryos (F,I), *Lefty2* expression is not detected, whereas the expression of *Lefty1* is restricted to the posterior floor plate. (J-L) *Pitx2* is expressed in left lateral mesoderm (arrow) of 12- to 14-somite stage *Cited2* wild-type (J) and heterozygous (K), but not *Cited2*-null (L) embryos. (M-R) At 13.5 dpc, *Pitx2* is expressed in the ventral myocardium of the right ventricle, throughout the left atrium and in ventrally viewed veins of *Cited2* wild-type embryos (M,P) and in null embryos that lack a laterality defect (N,Q). *Pitx2* is not expressed in the hearts of *Cited2*-null embryos that have a right isomeric phenotype (O,R). In some *Cited2*-null hearts, a novel domain of *Pitx2* expression was observed in dorsal ventricular cells (Q; arrow). Ventral view (A-C,J-O), lateral view (D-F), posterior view (G-I), dorsal view (P-R). Scale bar: 235 μm in A-C; 175 μm in D-I; 365 μm in J-L; 335 μm in M-R.

null (*n*=6) embryos that lacked laterality defects (Fig. 3M,N,P,Q; data not shown). By contrast, expression could not be detected in the hearts of *Cited2*-null embryos with right isomerism (*n*=7; Fig. 3O,R). Intriguingly, some *Cited2*-null hearts displayed a novel expression domain on the dorsal ventricular surface irrespective of their laterality phenotype (*n*=4/13; Fig. 3Q; data not shown).

Cited2-null embryos develop a spectrum of severe cardiovascular defects

Some cardiovascular defects that occur in *Cited2*-null embryos have previously been reported (Bamforth et al., 2001; Yin et al., 2002). Yet, the full spectrum of defects, their incidence and association to one another has remained unexplored. As *Cited2*-null embryos die late in gestation (Table 1) we examined a total of 28 *Cited2*-null embryos on a mixed C57Bl6;129 genetic background between 14.5 and 15.5 dpc using high-resolution images obtained from EFIC and 3D models (Weninger and Mohun, 2002). This revealed that *Cited2*-null embryos showed a broad range of cardiac, vascular and other defects, and were classified into four groups based on the predominant cardiac defect (Table 2). The major defect of group 1 embryos is right isomerism, the other abnormalities being largely attributable to the patterning defects that isomerism would impart. The incidence of isomerism in 14.5-15.5 dpc hearts is consistent with our finding that ~40% of embryos examined between 8.5 and 12.5 dpc have a laterality defect. As embryos in groups 2 to 4 do not show isomerism, the spectrum of cardiovascular defects they exhibit are likely to result from other factors, such as the reduction of CNC cells, or the lack of *Cited2* expression in cardiac tissues.

Cardiovascular defects associated with right isomerism

Nine out of 28 embryos (group 1; Table 2) demonstrated RPI and RAI as a component of a complex cardiac phenotype (compare Fig. 4A-C with 4D-F, Fig. 5A,C with 5B,D). Three-dimensional reconstruction of these *Cited2*-null hearts shows symmetrical arrangement of the atria, superior venae cavae and pulmonary veins (Fig. 6; Fig. 7A,B). A single common atrium is apparent with rudimentary ridges protruding into the lumen from the dorsal side. Both atrial appendages resemble the appearance of the normal right atrium (Figs 6-8). The superior venae cavae and inferior vena cava, along with multiple small mediastinal veins and a common pulmonary vein, drain into the central atrial area, which is bordered by the rudimentary ridges (Fig. 4B,G,H; Fig. 6C). In three embryos, an extra vessel (possibly a persisting right umbilical vein) enters the central atrial compartment from the caudal aspect (Fig. 6C′).

In six out of nine group 1 embryos, the common atrium was connected to a single ventricle with the inflow tract of the hypoplastic ventricle obstructed by the septal leaflet of a common AV valve (Fig. 4G; Fig. 8A,B,D,D′). In three out of nine group 1 embryos with an AV canal defect, there was a large VSD immediately beneath the AV junction. As a result, the common atrium opened equally into both ventricles (Fig. 4H). VSDs were apparent in three distinct sites: directly beneath the origin of the great vessels (outflow), beneath the AV junction (inflow) (Fig. 7C,C′; compare Fig. 4A,B with 4D,E, respectively), and near the apex cordis. Isomeric group 1 embryos also exhibited ventriculoarterial discordance and aortic arch anomalies. The abnormal arrangement of the great vessels and the ventricular chambers was manifest as either transposition of the great arteries (TGA) or DORV (data not shown). Aortic arch anomalies affected derivatives of the fourth and sixth arch arteries, and included interrupted aortic arch type B (IAA type B; Fig. 5, compare A and C with B and D), aberrant (retro-esophageal) right subclavian artery (Fig. 4I), and abnormalities of the size and position of the ductus arteriosus (data not shown).

In summary, nine out of 28 *Cited2*-null embryos examined have a right isomeric pulmonary and cardiac phenotype in combination with defects of the AV junction, ventricular septum, outflow tract and aortic arches. Each lesion (except for the muscular VSD) has previously been reported in association with aberrant left-right embryonic patterning (see Maclean and Dunwoodie, 2004; Schneider and Brueckner, 2000).

Cardiovascular defects in the absence of isomerism

Isomerism was not evident in the 15/28 *Cited2*-null embryos (Table 2). Group 2 embryos exhibited similar defects as those in group 1 but lack right isomerism. Group 3 defects were restricted to outflow tract malformations (DORV, TGA and overriding aorta) frequently in combination with muscular VSDs. Three *Cited2*-null embryos had multiple VSDs only (group 4), and a further four had a normal cardiac phenotype.

Endocardial cushions have reduced cell density in *Cited2*-null hearts

Cited2 is expressed in myocardium adjacent to endocardial cushions of the outflow tract and AV canal, and in some endocardial and cushion cells (Fig. 1I,J,N,Q). In addition, defects in endocardial cushions were detected at 14.5 dpc in *Cited2*-null embryos (Fig. 4G; Fig. 8A,B,D,D′). Therefore, we

Table 2. Phenotypic classification of *Cited2*-null embryos

	Group 1 (*n*=9)	Group 2 (*n*=4)	Group 3 (*n*=8)	Group 4 (*n*=3)
Right pulmonary isomerism	9			
Right atrial isomerism	9			
ASD	9, common atrium	4, foramen primum		
AV junction	9, common AV canal	4, common AV canal, DILV		
VSD	9, membranous, muscular	4, membranous, muscular	6, membranous, muscular	3, membranous, muscular
Outflow tract	9, DORV, TGA	4, DORV, PTA	8, DORV, TGA, OA	
Pharyngeal arch arteries	9, RERSA, IAA type B	4, RERSA, IAA type B		

A total of 28 embryos were analysed by EFIC and scored for phenotype of the cardiovascular system and lungs. Four embryos showed normal cardiovascular and pulmonary structure and the remaining 24 were classified into four groups by severity of phenotype. ASD, atrial septal defect; AV, atrioventricular; VSD, ventricular septal defects; DILV, double inlet left ventricle; DORV, double outlet left ventricle; TGA, transposition of the great arteries; PTA, persistent truncus arteriousus; OA, overriding aorta; RERSA, retro-esophogeal right subclavian artery; IAA, interrupted aortic arch.

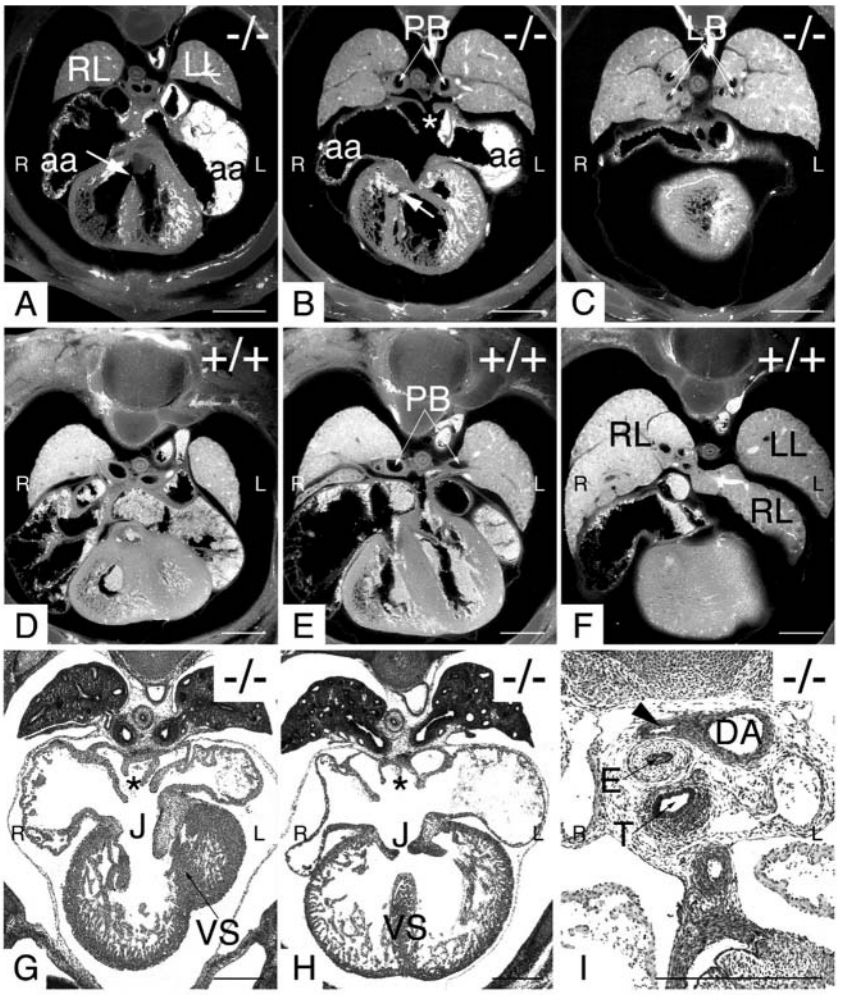

Fig. 4. *Cited2*-null embryos show a range of pulmonary and cardiac defects. Two dimension EFIC sections at 14.5 dpc through corresponding planes of a *Cited2*-null embryo (A-C) and a wild type (D-F) embryo. *Cited2*-null embryos show symmetrical arrangement of lung lobes, similar symmetry is evident in the size, topology and branching of the left and right principal bronchus (PB) and lobar bronchi (LB). *Cited2*-null embryos show cardiac defects that include a ventricular septal defect (arrows in A and B) and symmetrical right and left atrial appendages (aa) adjoining a median chamber (asterisk in B). Histological sections of 14.5 dpc *Cited2*-null embryos (G,H) show subtypes of atrioventricular junction (J) malformations: (G) single atrioventricular ostium opening solely into the right ventricle, (H) single atrioventricular ostium opening equally into both ventricles because of the large ventricular septal defect. The median atrial chamber is indicated by an asterisk. (I) Retro-esophageal right subclavian artery (arrowhead). E, esophagus; T, trachea; DA, descending aorta; VS, ventricular septum; R, right; L, left. Scale bar: 500 μm in A-F; 500 μm in G-I.

examined formation of endocardial cushions of the AV canal at 10.5 dpc (Fig. 9). The average cell density was significantly reduced (P<0.0001) in *Cited2*-null hearts (1.83×10^{-3} cells/μm^2±0.18×10^{-3}) compared with that in wild-type hearts (2.68×10^{-3} cells/μm^2± 0.15×10^{-3}) (compare Fig. 9E with 9F-H). Furthermore, the area of the endocardial cushions appeared to be reduced in the *Cited2*-null hearts, this is despite the fact that the overall sizes of the hearts compared were comparable.

Discussion

Here, we present a description of the full spectrum of cardiac defects that occur when the *Cited2* gene is absent during development. This analysis has revealed that right isomerism is a feature of the *Cited2*-null phenotype, and thus has lead to the finding that *Cited2* is required for correct specification of the left-right axis. In addition, the previously undefined expression profile of *Cited2*, in the developing heart and in tissues relevant to heart development, has been revealed. Collectively, these data demonstrate that the spectrum of cardiac defects is consistent with *Cited2* functioning at a number of levels to impact on heart development; these include a role for *Cited2* in establishment of the left-right axis, both directly in cardiac tissue and, as previously suggested, in cardiac neural crest cells.

A range of cardiac defects is observed in *Cited2*-null embryos. This variability in expressivity/penetrance of the phenotype is probably due to the effect(s) that polymorphism of a modifier(s) has on *Cited2* function. For example, the incidence of right isomerism occurs in about 33% of *Cited2*-null embryos with the 129/Olac;C57BL/6 genetic background compared with about 50% when the mixed SJL;C57BL/6 genetic background of the *MLC3F-nlacZ-2E* transgene is introduced.

Cited2 and the establishment of laterality

Establishment of left-right patterning can be divided into three phases: an initial break in embryonic symmetry through cilia-dependent processes originating in the node; establishment of asymmetric gene expression in lateral mesoderm; and transfer of positional information to developing organs. The Nodal signaling pathway, which is central to this process in the lateral mesoderm, is an important predictor of the phenotype (Collignon et al., 1996; Lowe et al., 1996). For example, left-sided expression results in situs solitus, right-sided expression in situs inversus, bilateral expression in left isomerism and absent expression in right isomerism.

The laterality defect in *Cited2*-null embryos is characterized by right atrial and RPI (100% concordant), and 50% of these individuals have altered abdominal situs. In addition, right atrial isomerism always occurs where the heart is abnormally looped. As *Cited2* is expressed in and around the ventral node, it is possible that Cited2 is required for cilia-dependent processes or for the relay of the asymmetric signal to the lateral mesoderm. Mutation in *Dnah5*, *Dnah11/Lrd*, *Hfh4/Foxj1* results in immotile cilia of the node, random expression of *Nodal* and the complete spectrum of laterality phenotypes: situs solitus, situs inversus, left and right isomerism (Brody et al., 2000; Chen et al., 1998; Collignon et al., 1996; Lowe et al., 1996; Meno et al., 1996; Oh and Li, 2002; Olbrich et al.,

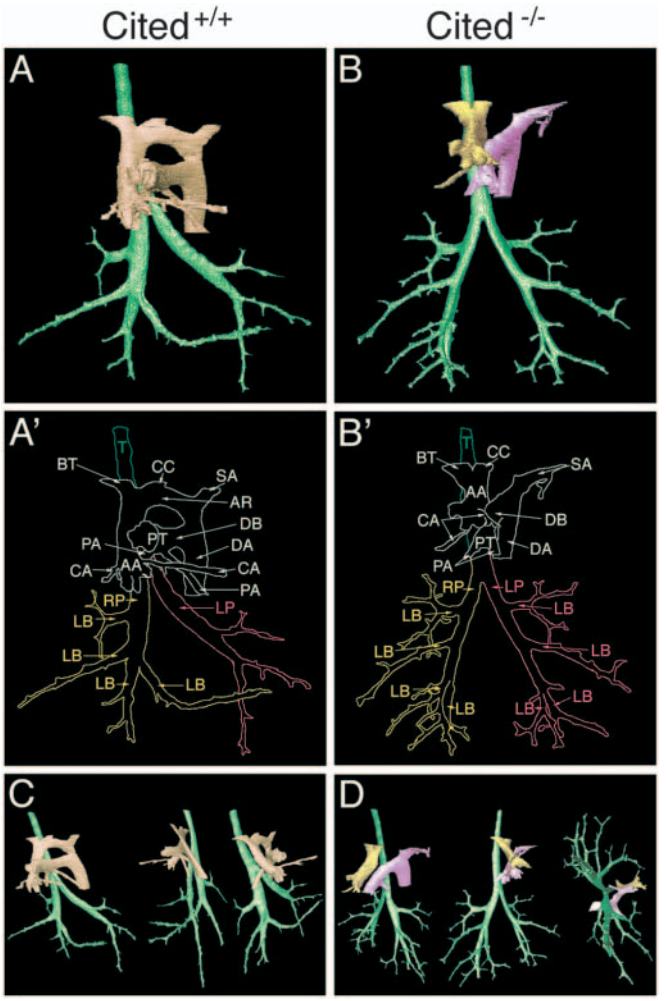

Fig. 5. Three-dimensional models of the bronchial system and great arteries, illustrating the right isomeric phenotype of *Cited2*-null embryos at 14.5 dpc. Models viewed from ventral (A,B) or left and right sides (C,D). (A,A′) Differences in topology, size, course and branching pattern of the right (yellow) and left (red) bronchial trees in the normal embryo, as well as in the arrangement of the blood vessels (brown). The *Cited2*-null embryo shows a symmetrical bronchial tree (B,B′), profound differences in the relationship between the bronchi and pulmonary arteries; transposition of the great arteries and interruption of the aortic arch between the origin of the left common carotid artery (CC) and the left subclavian artery (SA). (B,D) The pulmonary trunk, pulmonary arteries, ductus arteriosus, descending aorta, and left subclavian artery are shown in magenta; the aorta, coronary arteries, brachiocephalic trunk, and left common carotid artery are shown in gold. AA, ascending aorta; AR, aortic arch; DA, descending aorta; PT, pulmonary trunk; PA, pulmonary artery; DB, ductus arteriosus; CA, coronary artery; BT, brachiocephalic trunk; T, trachea; LB, lobar bronchus.

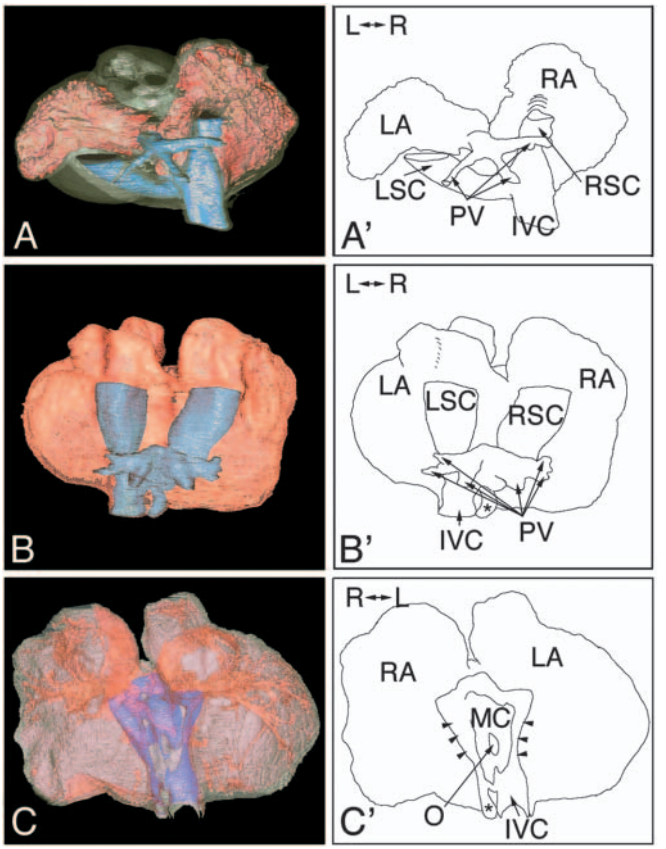

Fig. 6. Three-dimensional models (A-C) and labeled diagrams (A′-C′) showing atrial malformations of *Cited2*-null embryo hearts at 14.5 dpc. The models show the dorsal side of the atria (orange) and associated blood vessels (blue). (A,A′) Normal, asymmetric atrial appendages. (B,B′) *Cited2*-null hearts show symmetrical atrial appendages, each resembling a normal right atrium. The left superior vena cava (LSC) of the *Cited2*-null heart does not undercross the common space formed by pulmonary veins (PV): the symmetric arrangement of the pulmonary veins and the additional blood vessel (asterisk) to the right of the inferior vena cava (IVC). (C,C′) Dorsal atrial wall from the ventral aspect of a *Cited2*-null heart, after removal of the ventricles and atrioventricular junction from the model. Between the left and right atrial appendages, there is a median chamber (MC, purple) that is incompletely separated from them by ridges protruding from the dorsal side (arrowheads), this MC receives all veins. RA, right atrial appendage; LA, left atrial appendage; RSC, right superior vena cava; O, orifice of the lung vein.

2002; Supp et al., 1999; Supp et al., 1997). Moreover, mutations in genes that abrogate all nodal cilia (*Kif3a*, *Kif3b*, polaris, *Wim*) or just the sensory cilia (polycistin 2) result in absent, or bilateral *Nodal* expression that would result in situs inversus and left isomerism (Huangfu et al., 2003; Marszalek et al., 1999; Morgan et al., 1998; Moyer et al., 1994; Murcia et al., 2000; Nonaka et al., 1998; Pennekamp et al., 2002; Takeda et al., 1999; Wu et al., 2000). As *Cited2*-null embryos exhibit only situs solitus or right isomerism, it is unlikely that this gene is required only for cilia-dependent processes of the node and the breaking of embryonic symmetry.

Consistent with Nodal acting as a left-sided determinant, we have shown that complete absence of *Nodal* expression in lateral mesoderm is predictive of the right isomeric phenotype in *Cited2*-null embryos. This lack of *Nodal* suggests that *Cited2* is required for either the initiation or maintenance of *Nodal* expression, and thus requires *Cited2* to be expressed in lateral mesoderm. Appropriately, we have demonstrated low-level bilateral expression of *Cited2* in mouse LPM and we suggest that it acts in this tissue to initiate or maintain *Nodal* expression.

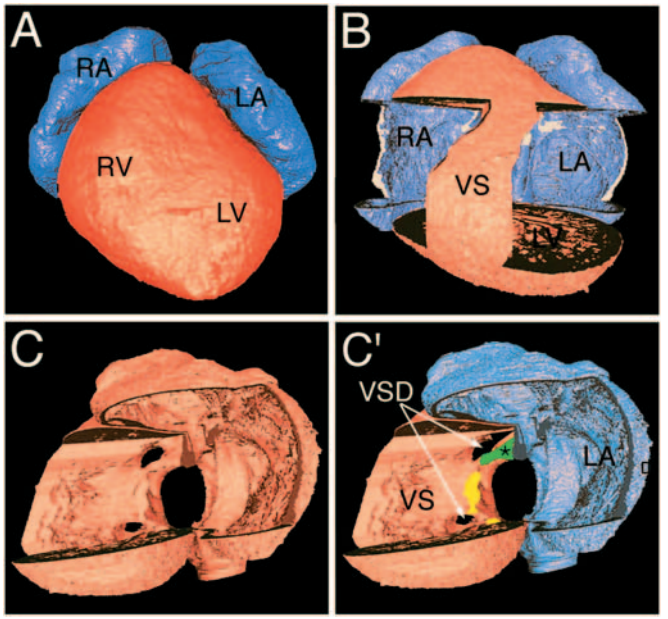

Fig. 7. Ventricular septal defects in *Cited2*-null embryos. (A) Three-dimensional model of a 14.5 dpc *Cited2*-null heart, viewed from the ventral side. (B) Ventral aspect, after removal of the ventral and lateral walls of the ventricles, up to (but not including) the ventricular septum (VS). The ventral and lateral walls of the atrial chambers have also been removed. The right ventricle has only a small volume. (C,C′) Model of (B) after 90° rotation (viewed from the left). A ventricular septal defect (VSD) is evident beneath the outflow tract, above the endocardardial cushion material (green, asterisk). A second VSD can be seen beneath the free margin of the septal leaflet (yellow) of the single atrioventricular valve. RA, right atrium; LA, left atrium; RV, right ventricle; LV, left ventricle.

It is not clear how loss of *Cited2* might affect *Nodal* expression. Cited2 binds CBP/p300, Tfap2 and Lhx2/3, and through its interaction with CBP/p300 affects the transcriptional activity of Hif1 and Ets1 (Bamforth et al., 2001; Braganca et al., 2002; De Guzman et al., 2004; Freedman et al., 2003; Glenn and Maurer, 1999; Yahata et al., 2000; Yokota et al., 2003). Investigation of the known Cited2-binding proteins sheds no light on its function, as mutations in these genes are not associated with laterality defects (Barton et al., 1998; Goodman and Smolik, 2000; Iyer et al., 1998; Ryan et al., 1998; Schorle et al., 1996; Shikama et al., 2003; Zhang et al., 1996).

The expression of *Lefty1* and *Lefty2* is abnormal in a proportion of *Cited2*-null embryos. Consistent with the loss of *Nodal* expression in the left LPM, *Lefty2* expression was not detected. In addition, *Lefty1* expression was largely not detected in the left PFP as the loss of *Nodal* expression in the left LPM might predict. Intriguingly, however, *Lefty1* expression was readily detected in the posterior PFP. Regulatory elements directing anterior and posterior expression of *Lefty1* and *Lefty2* have been identified (Saijoh et al., 1999), and so it is possible that *Cited2,* directly or indirectly, acts through an enhancer that controls the anterior, but not posterior, expression of *Lefty1*.

A proportion of *Cited2*-null embryos do not express *Pitx2c* in left lateral mesoderm, or in right isomeric hearts at later

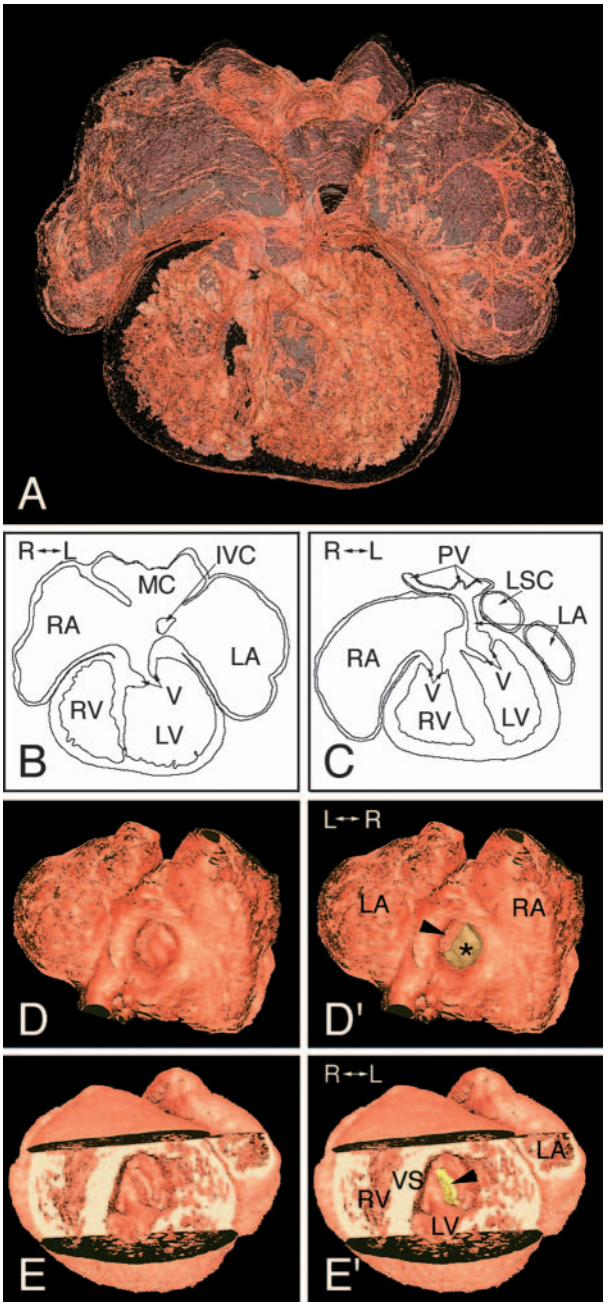

Fig. 8. Malformations in the atrioventricular junction of *Cited2*-null embryos. (A) Semi-transparent view of a 14.5 dpc *Cited2*-null heart, annotated in B. The cranial parts of the ventricles and atria have been removed from the model. A single atrioventricular ostium opens solely into the left ventricle (LV), guarded by leaflets (V) of a single atrioventricular valve. (C) An equivalent view obtained by modeling a normal heart. (D,D′) Atrioventricular junction of a *Cited2*-null embryo, seen from the atrium after removal of the dorsal atrial wall. The atrioventricular valve has only one leaflet (brown, asterisk) and the opens into the left ventricle (arrowhead). (E,E′) Atrioventricular junction of a *Cited2*-null heart, viewed from ventral side after removal of the apical parts of the ventricle walls and the ventricle septum (VS). The right (RV) and left (LV) ventricle differ in volume and there is only a single opening of the atrioventricular ostium (yellow, arrowhead) into the LV. LA, left atrium; RA, right atrium; MC, median chamber of atrium; PV, pulmonary vein; LSC, left superior vena cava; IVC, inferior vena cava; R L, right-left axis.

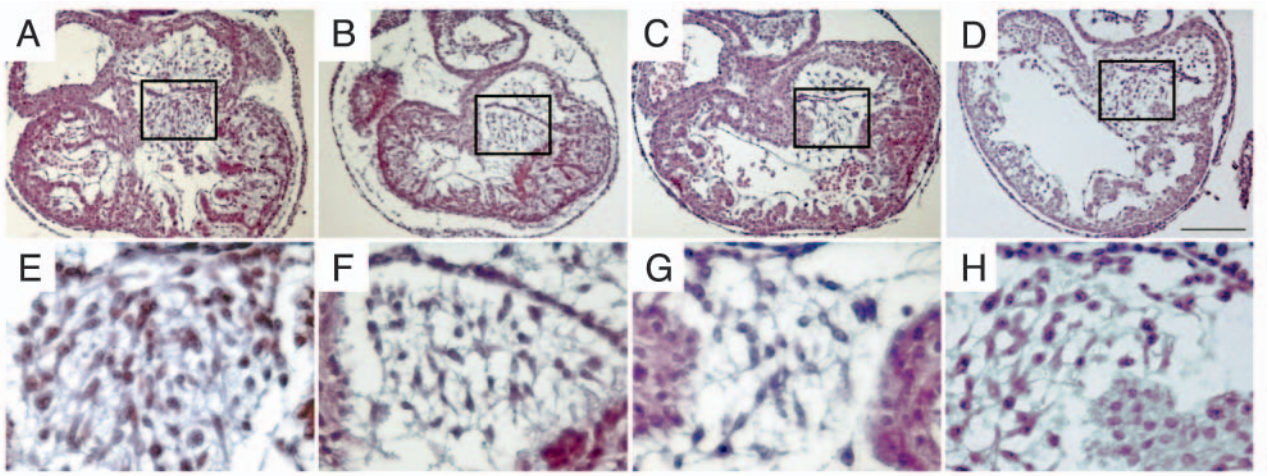

Fig. 9. *Cited2*-null embryos have reduced cell density of the atrioventricular cushions. Hematoxylin and Eosin-stained sections of *Cited2* wild-type (A,E) and null embryos (B-D,F-H) at 10 dpc. Sections were cut at a 45° angle (midway between frontal and transverse). (E-H) Higher magnifications of the boxed regions in A-D, showing the reduced cell density within the atrioventricular cushions in the *Cited2*-null hearts. Scale bar: 285 μm in A-D; 75 μm in E-H.

stages of development. This may simply reflect the fact that *Pitx2c* expression requires Nodal signaling, and that *Nodal* is not expressed in *Cited2*-null embryos with laterality defects. This assumes that *Pitx2c* expression in the heart requires prior expression of *Pitx2c* in the lateral mesoderm. No evidence contradictory to this exists, and the fact that expression of *Pitx2c* in the anterior lateral mesoderm at 8.5 dpc is consistent with the sites of *Pitx2c* expression in the heart at later stages (13.5-14.5 dpc) supports this hypothesis (Campione et al., 2001). In addition, there are no cases in which *Pitx2c* expression is observed in the heart in the absence of prior expression in the anterior lateral mesoderm.

It is possible that *Pitx2c* expression in the heart has little to do with prior gene activation by Nodal, and that Cited2 might have a more direct role in its expression. This hypothesis is supported by the overlapping expression patterns of *Cited2* and *Pitx2c*; both are expressed in the primary atrial septum, pulmonary veins and superior vena cava. In addition, they are expressed in the atrial myocardium, AV canals and outflow tract, although *Pitx2c* is only expressed on the left side of these structures (Campione et al., 2001; Franco and Campione, 2003; Franco et al., 2000). Furthermore, embryos null for either *Cited2* or *Pitx2c* develop similar cardiac defects (Franco and Campione, 2003; Liu et al., 2001).

A very recent report proposes that *Cited2* acts directly upstream of *Pitx2c*, and that the severe and complex heart defects apparent in *Cited2*-null embryos, that lack a laterality defect, occur because Cited2 is required to directly activate *Pitx2c* expression in the heart (Bamforth et al., 2004). This hypothesis seems unlikely for the following reasons. First, Bamforth et al. (Bamforth et al., 2004) show that the activity of the *Pitx2*c P1 promoter can be increased by about 1.5-fold following co-transfection of *Cited2* and the A and C isoforms of transcription factor *Tfap2* (in the hepatoma cell line Hep3B cells). However, the degree of transactivation is slight in comparison with a 25-fold increase in activation of the same promoter fragment through the Nodal-responsive Fast1/Foxh1 binding sites (Shiratori et al., 2001). This suggests that if Cited2-Tfap2a/c activates *Pitx2c* expression in the heart, it does so at relatively low levels and thus is not a major determinant of *Pitx2c* expression.

In addition, if the Cited2-Tfap2a/c complex activates *Pitx2c* in the heart, one would expect in *Cited2*-null embryos where laterality is normally established (and *Pitx2c* is expressed in left lateral mesoderm) that *Pitx2c* expression would be greatly reduced or absent in the heart. Evidence supporting this was not provided by Bamforth et al. (Bamforth et al., 2004): three *Cited2*-null hearts of a mixed genetic background (C57BL6/J;129Sv) were examined for *Pitx2c* expression, one showed reduced expression; however, the laterality status of these hearts was not determined. By contrast, we find that *Pitx2c* expression in the heart is coupled with its expression in lateral mesoderm: *Cited2*-null embryos with right isomerism lack *Pitx2c* expression in the left lateral mesoderm and in the heart; those without a laterality defect express *Pitx2c* in both left lateral mesoderm and the heart. Our data thus argues against Cited2 playing a direct and major role in the expression of *Pitx2c* in the heart, and instead supports the hypothesis that loss of *Pitx2c* in the heart occurs only when this gene is not expressed in the left lateral mesoderm at an earlier developmental stage. Importantly, the *Cited2*-null embryos, which express *Pitx2c* in the heart, still develop a complex array of cardiac defects, indicating that *Cited2* expression is required in the heart for normal development and that it has *Pitx2c*-independent functions.

Cited2, heterotaxia and congenital heart disease

Our studies of the *Cited2*-null phenotype in the mouse demonstrate that mutation of a single gene can result in a remarkably wide spectrum of cardiac malformations. To date, no mutations have been identified in *CITED2* in human disorders; however, the right isomeric phenotype of *Cited2*-null embryos resembles that seen in some individuals with heterotaxia and, in particular, asplenia (Ivemark) syndrome (OMIM 208530) (Ivemark, 1955). In humans, heterotaxia is a clinically and genetically heterogeneous disorder that is associated with a broad range of cardiac malformations. It occurs in approximately one in 10,000 live born infants or 1%

of children with congenital heart disease, and common cardiac manifestations are complex, including TGA, DORV or AV septal defects (Hutchins et al., 1983; Rose et al., 1975; Ruttenberg et al., 1964; Van Mierop and Wiglesworth, 1962). Thus, the *Cited2*-null embryo provides a useful model with which to investigating the etiology of heterotaxia in humans. Furthermore, as the *Cited2* mutation results in a spectrum of phenotypes that vary widely in their severity, it raises the possibility that many less severe congenital heart defects share a common cause with each other and with heterotaxia.

We thank Margaret Buckingham and Robert Kelly for the MLC3F-*nlacZ*-2E mice; Christine Biben and Richard Harvey for the *Nodal*, *Lefty1/2* and *Pitx2* cDNA probes and for many helpful discussions; and Richard Harvey, Ken Maclean and Duncan Sparrow for critical assessment of the manuscript. K.L.F. is a recipient of an Australian Postgraduate Award. S.L.W. is a Royal Society of London International Postdoctoral Fellow and a Wellcome Trust International Travelling Research Fellow. S.L.D. is a Pfizer Foundation Australia Senior Research Fellow.

References

Bamforth, S. D., Braganca, J., Eloranta, J. J., Murdoch, J. N., Marques, F. I., Kranc, K. R., Farza, H., Henderson, D. J., Hurst, H. C. and Bhattacharya, S. (2001). Cardiac malformations, adrenal agenesis, neural crest defects and exencephaly in mice lacking Cited2, a new Tfap2 co-activator. *Nat. Genet.* **29**, 469-474.

Bamforth, S. D., Braganca, J., Farthing, C. R., Schneider, J. E., Broadbent, C., Michell, A. C., Clarke, K., Neubauer, S., Norris, D., Brown, N. A. et al. (2004). Cited2 controls left-right patterning and heart development through a Nodal-Pitx2c pathway. *Nat. Genet.* **36**, 1189-1196.

Barbera, J. P., Rodriguez, T. A., Greene, N. D., Weninger, W. J., Simeone, A., Copp, A. J., Beddington, R. S. P. and Dunwoodie, S. (2002). Folic acid prevents exencephaly in Cited2 deficient mice. *Hum. Mol. Genet.* **11**, 283-293.

Barton, K., Muthusamy, N., Fischer, C., Ting, C. N., Walunas, T. L., Lanier, L. L. and Leiden, J. M. (1998). The Ets-1 transcription factor is required for the development of natural killer cells in mice. *Immunity* **9**, 555-563.

Bhattacharya, S., Michels, C. L., Leung, M. K., Arany, Z. P., Kung, A. L. and Livingston, D. M. (1999). Functional role of p35srj, a novel p300/CBP binding protein, during transactivation by HIF-1. *Genes Dev.* **13**, 64-75.

Braganca, J., Swingler, T., Marques, F. I., Jones, T., Eloranta, J. J., Hurst, H. C., Shioda, T. and Bhattacharya, S. (2002). Human CREB-binding protein/p300-interacting transactivator with ED-rich tail (CITED) 4, a new member of the CITED family, functions as a co-activator for transcription factor AP-2. *J. Biol. Chem.* **277**, 8559-8565.

Brody, S. L., Yan, X. H., Wuerffel, M. K., Song, S. K. and Shapiro, S. D. (2000). Ciliogenesis and left-right axis defects in forkhead factor HFH-4-null mice. *Am. J. Respir. Cell Mol. Biol.* **23**, 45-51.

Burdine, R. D. and Schier, A. F. (2000). Conserved and divergent mechanisms in left-right axis formation. *Genes Dev.* **14**, 763-776.

Campione, M., Ros, M. A., Icardo, J. M., Piedra, E., Christoffels, V. M., Schweickert, A., Blum, M., Franco, D. and Moorman, A. F. (2001). Pitx2 expression defines a left cardiac lineage of cells: evidence for atrial and ventricular molecular isomerism in the iv/iv mice. *Dev. Biol.* **231**, 252-264.

Chan, H. M. and la Thangue, N. B. (2001). p300/CBP proteins: HATs for transcriptional bridges and scaffolds. *J. Cell Sci.* **114**, 2363-2373.

Chen, C. and Shen, M. M. (2004). Two modes by which Lefty proteins inhibit nodal signaling. *Curr. Biol.* **14**, 618-624.

Chen, J., Knowles, H. J., Hebert, J. L. and Hackett, B. P. (1998). Mutation of the mouse hepatocyte nuclear factor/forkhead homologue 4 gene results in an absence of cilia and random left-right asymmetry. *J. Clin. Invest.* **102**, 1077-1082.

Cheng, S. K., Olale, F., Brivanlou, A. H. and Schier, A. F. (2004). Lefty blocks a subset of TGFbeta signals by antagonizing EGF-CFC coreceptors. *PLoS Biol* **2**, E30.

Collignon, J., Varlet, I. and Robertson, E. J. (1996). Relationship between asymmetric nodal expression and the direction of embryonic turning. *Nature* **381**, 155-158.

De Guzman, R. N., Martinez-Yamout, M. A., Dyson, H. J. and Wright, P. E. (2004). Interaction of the TAZ1 domain of the CREB-binding protein with the activation domain of CITED2: regulation by competition between intrinsically unstructured ligands for non-identical binding sites. *J. Biol. Chem.* **279**, 3042-3049.

Dunwoodie, S. L., Rodriguez, T. A. and Beddington, R. S. (1998). Msg1 and Mrg1, founding members of a gene family, show distinct patterns of gene expression during mouse embryogenesis. *Mech. Dev.* **72**, 27-40.

Franco, D. and Campione, M. (2003). The role of Pitx2 during cardiac development. Linking left-right signaling and congenital heart diseases. *Trends Cardiovasc. Med.* **13**, 157-163.

Franco, D., Campione, M., Kelly, R., Zammit, P. S., Buckingham, M., Lamers, W. H. and Moorman, A. F. (2000). Multiple transcriptional domains, with distinct left and right components, in the atrial chambers of the developing heart. *Circ Res.* **87**, 984-991.

Franco, D., Kelly, R., Moorman, A. F., Lamers, W. H., Buckingham, M. and Brown, N. A. (2001). MLC3F transgene expression in iv mutant mice reveals the importance of left-right signalling pathways for the acquisition of left and right atrial but not ventricular compartment identity. *Dev. Dyn.* **221**, 206-215.

Freedman, S. J., Sun, Z. Y., Kung, A. L., France, D. S., Wagner, G. and Eck, M. J. (2003). Structural basis for negative regulation of hypoxia-inducible factor-1alpha by CITED2. *Nat. Struct. Biol.* **10**, 504-512.

Glenn, D. J. and Maurer, R. A. (1999). MRG1 binds to the LIM domain of Lhx2 and may function as a coactivator to stimulate glycoprotein hormone alpha-subunit gene expression. *J. Biol. Chem.* **274**, 36159-36167.

Goodman, R. H. and Smolik, S. (2000). CBP/p300 in cell growth, transformation, and development. *Genes Dev.* **14**, 1553-1577.

Grossman, S. R., Deato, M. E., Brignone, C., Chan, H. M., Kung, A. L., Tagami, H., Nakatani, Y. and Livingston, D. M. (2003). Polyubiquitination of p53 by a ubiquitin ligase activity of p300. *Science* **300**, 342-344.

Hamada, H., Meno, C., Watanabe, D. and Saijoh, Y. (2002). Establishment of vertebrate left-right asymmetry. *Nat. Rev. Genet.* **3**, 103-113.

Harrison, S. M., Dunwoodie, S. L., Arkell, R. M., Lehrach, H. and Beddington, R. S. (1995). Isolation of novel tissue-specific genes from cDNA libraries representing the individual tissue constituents of the gastrulating mouse embryo. *Development* **121**, 2479-2489.

Hogan, B., Beddington, R., Constantini, F. and Lacy, E. (1994). *Manipulating the Mouse Embryo. A Laboratory Manual.* New York: Cold Spring Harbor Laboratory Press.

Huangfu, D., Liu, A., Rakeman, A. S., Murcia, N. S., Niswander, L. and Anderson, K. V. (2003). Hedgehog signalling in the mouse requires intraflagellar transport proteins. *Nature* **426**, 83-87.

Hutchins, G. M., Moore, G. W., Lipford, E. H., Haupt, H. M. and Walker, M. C. (1983). Asplenia and polysplenia malformation complexes explained by abnormal embryonic body curvature. *Pathol. Res. Pract.* **177**, 60-76.

Ivemark, B. I. (1955). Implications of agenesis of the spleen on the pathogenesis of conotruncus anomalies in childhood; an analysis of the heart malformations in the splenic agenesis syndrome, with fourteen new cases. *Acta Paediatr.* **44**, 7-110.

Iyer, N. V., Kotch, L. E., Agani, F., Leung, S. W., Laughner, E., Wenger, R. H., Gassmann, M., Gearhart, J. D., Lawler, A. M., Yu, A. Y. et al. (1998). Cellular and developmental control of O2 homeostasis by hypoxia-inducible factor 1 alpha. *Genes Dev.* **12**, 149-162.

Kaufman, M. H. (1992). *The Atlas of Mouse Development*. London: Academic Press.

Kelly, R., Alonso, S., Tajbakhsh, S., Cossu, G. and Buckingham, M. (1995). Myosin light chain 3F regulatory sequences confer regionalized cardiac and skeletal muscle expression in transgenic mice. *J. Cell Biol.* **129**, 383-396.

Kelly, R. G., Zammit, P. S., Mouly, V., Butler-Browne, G. and Buckingham, M. E. (1998). Dynamic left/right regionalisation of endogenous myosin light chain 3F transcripts in the developing mouse heart. *J. Mol. Cell Cardiol.* **30**, 1067-1081.

Liu, C., Liu, W., Lu, M. F., Brown, N. A. and Martin, J. F. (2001). Regulation of left-right asymmetry by thresholds of Pitx2c activity. *Development* **128**, 2039-2048.

Lowe, L. A., Supp, D. M., Sampath, K., Yokoyama, T., Wright, C. V., Potter, S. S., Overbeek, P. and Kuehn, M. R. (1996). Conserved left-right asymmetry of nodal expression and alterations in murine situs inversus. *Nature* **381**, 158-161.

Maclean, K. and Dunwoodie, S. (2004). Breaking symmetry: a clinical overview of left-right patterning. *Clin. Genet.* **65**, 441-457.

Marszalek, J. R., Ruiz-Lozano, P., Roberts, E., Chien, K. R. and Goldstein, L. S. (1999). Situs inversus and embryonic ciliary morphogenesis defects in mouse mutants lacking the KIF3A subunit of kinesin-II. *Proc. Natl. Acad. Sci. USA* **96**, 5043-5048.

Martinez Barbera, J. P., Rodriguez, T. A., Greene, N. D., Weninger, W. J., Simeone, A., Copp, A. J., Beddington, R. S. P. and Dunwoodie, S. (2002). Folic acid prevents exencephaly in Cited2 deficient mice. *Hum. Mol. Genet.* **11**, 283-293.

Meno, C., Saijoh, Y., Fujii, H., Ikeda, M., Yokoyama, T., Yokoyama, M., Toyoda, Y. and Hamada, H. (1996). Left-right asymmetric expression of the TGF beta-family member lefty in mouse embryos. *Nature* **381**, 151-155.

Meno, C., Ito, Y., Saijoh, Y., Matsuda, Y., Tashiro, K., Kuhara, S. and Hamada, H. (1997). Two closely-related left-right asymmetrically expressed genes, lefty-1 and lefty-2: their distinct expression domains, chromosomal linkage and direct neuralizing activity in Xenopus embryos. *Genes Cells* **2**, 513-524.

Morgan, D., Turnpenny, L., Goodship, J., Dai, W., Majumder, K., Matthews, L., Gardner, A., Schuster, G., Vien, L., Harrison, W. et al. (1998). Inversin, a novel gene in the vertebrate left-right axis pathway, is partially deleted in the inv mouse. *Nat. Genet.* **20**, 149-156.

Moyer, J. H., Lee-Tischler, M. J., Kwon, H. Y., Schrick, J. J., Avner, E. D., Sweeney, W. E., Godfrey, V. L., Cacheiro, N. L., Wilkinson, J. E. and Woychik, R. P. (1994). Candidate gene associated with a mutation causing recessive polycystic kidney disease in mice. *Science* **264**, 1329-1333.

Murcia, N. S., Richards, W. G., Yoder, B. K., Mucenski, M. L., Dunlap, J. R. and Woychik, R. P. (2000). The Oak Ridge Polycystic Kidney (orpk) disease gene is required for left-right axis determination. *Development* **127**, 2347-2355.

Nonaka, S., Tanaka, Y., Okada, Y., Takeda, S., Harada, A., Kanai, Y., Kido, M. and Hirokawa, N. (1998). Randomization of left-right asymmetry due to loss of nodal cilia generating leftward flow of extraembryonic fluid in mice lacking KIF3B motor protein. *Cell* **95**, 829-837.

Oh, S. P. and Li, E. (2002). Gene-dosage-sensitive genetic interactions between inversus viscerum (iv), nodal, and activin type IIB receptor (ActRIIB) genes in asymmetrical patterning of the visceral organs along the left-right axis. *Dev. Dyn.* **224**, 279-290.

Olbrich, H., Haffner, K., Kispert, A., Volkel, A., Volz, A., Sasmaz, G., Reinhardt, R., Hennig, S., Lehrach, H., Konietzko, N. et al. (2002). Mutations in DNAH5 cause primary ciliary dyskinesia and randomization of left-right asymmetry. *Nat. Genet.* **30**, 143-144.

Pennekamp, P., Karcher, C., Fischer, A., Schweickert, A., Skryabin, B., Horst, J., Blum, M. and Dworniczak, B. (2002). The ion channel polycystin-2 is required for left-right axis determination in mice. *Curr. Biol.* **12**, 938-943.

Rose, V., Izukawa, T. and Moes, C. A. (1975). Syndromes of asplenia and polysplenia. A review of cardiac and non-cardiac malformations in 60 cases with special reference to diagnosis and prognosis. *Br. Heart J.* **37**, 840-852.

Ruttenberg, H. D., Neufeld, H. N., Lucas, R. V., Jr, Carey, L. S., Adams, P., Jr, Anderson, R. C. and Edwards, J. E. (1964). Syndrome of congenital cardiac disease with asplenia. distinction from other forms of congenital cyanotic cardiac disease. *Am. J. Cardiol.* **13**, 387-406.

Ryan, H. E., Lo, J. and Johnson, R. S. (1998). HIF-1 alpha is required for solid tumor formation and embryonic vascularization. *EMBO J.* **17**, 3005-3015.

Saijoh, Y., Adachi, H., Mochida, K., Ohishi, S., Hirao, A. and Hamada, H. (1999). Distinct transcriptional regulatory mechanisms underlie left-right asymmetric expression of lefty-1 and lefty-2. *Genes Dev.* **13**, 259-269.

Saijoh, Y., Adachi, H., Sakuma, R., Yeo, C. Y., Yashiro, K., Watanabe, M., Hashiguchi, H., Mochida, K., Ohishi, S., Kawabata, M. et al. (2000). Left-right asymmetric expression of lefty2 and nodal is induced by a signaling pathway that includes the transcription factor FAST2. *Mol. Cell* **5**, 35-47.

Schlange, T., Andree, B., Arnold, H. and Brand, T. (2000). Expression analysis of the chicken homologue of CITED2 during early stages of embryonic development. *Mech. Dev.* **98**, 157-160.

Schneider, H. and Brueckner, M. (2000). Of mice and men: dissecting the genetic pathway that controls left-right asymmetry in mice and humans. *Am. J. Med. Genet.* **97**, 258-270.

Schorle, H., Meier, P., Buchert, M., Jaenisch, R. and Mitchell, P. J. (1996). Transcription factor AP-2 essential for cranial closure and craniofacial development. *Nature* **381**, 235-238.

Shikama, N., Lutz, W., Kretzschmar, R., Sauter, N., Roth, J. F., Marino, S., Wittwer, J., Scheidweiler, A. and Eckner, R. (2003). Essential function of p300 acetyltransferase activity in heart, lung and small intestine formation. *EMBO J.* **22**, 5175-5185.

Shiratori, H., Sakuma, R., Watanabe, M., Hashiguchi, H., Mochida, K., Sakai, Y., Nishino, J., Saijoh, Y., Whitman, M. and Hamada, H. (2001). Two-step regulation of left-right asymmetric expression of Pitx2: initiation by nodal signaling and maintenance by Nkx2. *Mol. Cell* **7**, 137-149.

Sun, H. B., Zhu, Y. X., Yin, T., Sledge, G. and Yang, Y. C. (1998). MRG1, the product of a melanocyte-specific gene related gene, is a cytokine-inducible transcription factor with transformation activity. *Proc. Natl. Acad. Sci. USA* **95**, 13555-13560.

Supp, D. M., Brueckner, M., Kuehn, M. R., Witte, D. P., Lowe, L. A., McGrath, J., Corrales, J. and Potter, S. S. (1999). Targeted deletion of the ATP binding domain of left-right dynein confirms its role in specifying development of left-right asymmetries. *Development* **126**, 5495-5504.

Supp, D. M., Witte, D. P., Potter, S. S. and Brueckner, M. (1997). Mutation of an axonemal dynein affects left-right asymmetry in inversus viscerum mice. *Nature* **389**, 963-966.

Takeda, S., Yonekawa, Y., Tanaka, Y., Okada, Y., Nonaka, S. and Hirokawa, N. (1999). Left-right asymmetry and kinesin superfamily protein KIF3A: new insights in determination of laterality and mesoderm induction by kif3A$^{-/-}$ mice analysis. *J. Cell Biol.* **145**, 825-836.

Van Mierop, L. H. and Wiglesworth, F. W. (1962). Isomerism of the cardiac atria in the asplenia syndrome. *Lab. Invest.* **11**, 1303-1315.

Webb, S., Brown, N. A. and Anderson, R. H. (1998). Formation of the atrioventricular septal structures in the normal mouse. *Circ. Res.* **82**, 645-656.

Weninger, W. J. and Mohun, T. (2002). Phenotyping transgenic embryos: a rapid 3-D screening method based on episcopic fluorescence image capturing. *Nat. Genet.* **30**, 59-65.

Wu, G., Markowitz, G. S., Li, L., D'Agati, V. D., Factor, S. M., Geng, L., Tibara, S., Tuchman, J., Cai, Y., Park, J. H. et al. (2000). Cardiac defects and renal failure in mice with targeted mutations in Pkd2. *Nat. Genet.* **24**, 75-78.

Yahata, T., de Caestecker, M. P., Lechleider, R. J., Andriole, S., Roberts, A. B., Isselbacher, K. J. and Shioda, T. (2000). The MSG1 non-DNA-binding transactivator binds to the p300/CBP coactivators, enhancing their functional link to the Smad transcription factors. *J. Biol. Chem.* **275**, 8825-8834.

Yan, Y. T., Gritsman, K., Ding, J., Burdine, R. D., Corrales, J. D., Price, S. M., Talbot, W. S., Schier, A. F. and Shen, M. M. (1999). Conserved requirement for EGF-CFC genes in vertebrate left-right axis formation. *Genes Dev.* **13**, 2527-2537.

Yin, Z., Haynie, J., Yang, X., Han, B., Kiatchoosakun, S., Restivo, J., Yuan, S., Prabhakar, N. R., Herrup, K., Conlon, R. A. et al. (2002). The essential role of Cited2, a negative regulator for HIF-1alpha, in heart development and neurulation. *Proc. Natl. Acad. Sci. USA* **99**, 10488-10493.

Yokota, H., Goldring, M. B. and Sun, H. B. (2003). CITED2-mediated regulation of MMP-1 and MMP-13 in human chondrocytes under flow shear. *J. Biol. Chem.* **278**, 47275-47280.

Yoshioka, H., Meno, C., Koshiba, K., Sugihara, M., Itoh, H., Ishimaru, Y., Inoue, T., Ohuchi, H., Semina, E. V., Murray, J. C. et al. (1998). Pitx2, a bicoid-type homeobox gene, is involved in a lefty-signaling pathway in determination of left-right asymmetry. *Cell* **94**, 299-305.

Zhang, J., Hagopian-Donaldson, S., Serbedzija, G., Elsemore, J., Plehn-Dujowich, D., McMahon, A. P., Flavell, R. A. and Williams, T. (1996). Neural tube, skeletal and body wall defects in mice lacking transcription factor AP-2. *Nature* **381**, 238-241.